Assessment of Doppler effect on LoRa communication in 1U CubeSat: insights from MicroOrbiter-1 satellite

By Nova Maras Nurul KHAMSAH,[1)] Fahd MOUMNI,[1),2)] Edgar MUJUNI,[1)] Sirash SAYANJU,[1)] Yasir Mohamed Osman ABBAS,[2)] Jose Rodrigo Cordova ALARCON,[1)] Necmi Cihan ORGER,[1)] Victor Hugo SCHULZ,[1)] Daiki NOBAYASHI,[1)] Takeshi IKENAGA,[1)] Yoji HIRAKATA,[2)] and Mengu CHO[1)]

[1)] *Kyushu Institute of Technology, Kitakyushu, Japan*
[2)] *MicroOrbiter Inc., Tokyo, Japan*

The Integration of Long Range (LoRa) technology into CubeSat missions represents a significant advancement in small satellite communications. While LoRa is one of the promising technologies for Internet of Things (IoT) communication in a CubeSat due to its low power consumption, it remains susceptible to the Doppler effect especially in the lower orbit. This paper presents a comprehensive assessment of the Doppler effect on LoRa communication in a 1U CubeSat environment, based on real-time data from the MicroOrbiter-1 (MO-1) satellite mission. The study focuses on LoRa transmissions with Spreading Factors (SF) 7 and 10, using ground sensor terminals (GSTs) located in Japan and the United States. Through analysis of Doppler shift and rate effects on LoRa signals during various orbital passes, the impact on signal quality and overall communication reliability is examined. Key findings reveal LoRa modulation's resilience to Doppler effects in space, with notable observations of a correlation between the satellite's elevation angle and Doppler-induced signal degradation. This study provides empirical data on LoRa performance environments, offering insights for optimizing LoRa parameters in future CubeSat missions and demonstrating the viability of LoRa technology for small satellite communications.

Key Words: CubeSat, Doppler effect, LoRa, MicroOrbiter-1, satellite communication

Nomenclature

c	:	Speed of light, $3 \times 10^8 m/s$
f	:	frequency
f_c	:	Carrier frequency
f_s	:	Doppler shift
FSL	:	Free Space Loss, dB
G	:	Antenna Gain, dBi
I	:	Interference, dB
L	:	Losses, dB
P_{rx}	:	Received Power, dB
P_{tx}	:	Transmission Power, dB
$\vec{r}_{gs}$	:	position vector
$\vec{r}_{rel}$	:	relative position vector
t	:	time step, s
V_{rel}	:	Instantaneous relative radial velocity
$\vec{v}$	:	velocity vector
$\vec{v}_{rel}$	:	relative velocity vector
Subscripts		
ch	:	Channel
gst	:	Ground Sensor Terminal
sat	:	Satellite
sys	:	System

1. Introduction

The advent of CubeSats has revolutionized space exploration and communication, offering a cost-effective platform for various applications.[1)] Among these, satellite-based Internet of Things (IoT) systems have received significant attention due to their potential to provide connectivity in remote and undeserved regions. CubeSats, because of their scalability, are increasingly being considered as viable platforms for enabling global IoT coverage.

To explore this potential, recent studies have assessed the performance and applicability of CubeSat-based IoT architectures in real-world scenarios. Reference 2) evaluated the capacity and coverage of a CubeSat-enabled satellite IoT network, focusing on communication strategies tailored for developing countries.

As these small satellites become popular, the demand for reliable and efficient communication systems becomes increasingly prevalent. LoRa (Long Range) technology, originally designed for terrestrial Internet of Things (IoT) applications,[3)] has emerged as a promising solution for CubeSat communications due to its low power consumption and long-range capabilities.[4,5)] However, the implementation of LoRa in satellite communications faces unique challenges, particularly the Doppler effect.

This phenomenon, caused by the relative motion between the satellite and ground stations (GS) or ground sensor terminals (GSTs), can significantly affect signal quality and communication reliability. The Doppler effect in satellite communications manifests itself as a frequency shift in the received signal relative to the transmitted signal. For Low Earth Orbit (LEO) satellites, which typically operate at altitudes between 400 and 2000 km, the Doppler shift can be substantial because of their high velocity relative to earth-based transmitters and receivers.

LoRa employs a unique Chirp Spread Spectrum (CSS) modulation technique, which offers inherent resilience to frequency offsets. This characteristic makes LoRa potentially suitable for satellite communications, where Doppler shifts are inevitable. However, the extent of this resilience in the context of rapidly moving LEO satellites remains an area of active research.[6,7)]

Recent studies have investigated the performance of LoRa under various Doppler conditions. Reference 8) demonstrated that LoRa could maintain communication links with frequency offsets of up to 20% of the signal bandwidth. However, their work primarily focused on terrestrial applications, leaving room for further investigation in satellite scenarios. In Ref. 9), the Doppler effect in satellite LoRa communications is analyzed, highlighting the challenges of accurately predicting Doppler shifts induced by satellite motion and the need for sophisticated modeling techniques.

Another study in Ref. 10, 11) conducted a comprehensive study on the impact of the Doppler effect on the reliability of LoRa satellite links, distinguishing between the Doppler shift and the Doppler rate, and identifying key communication parameters that influence performance.

This paper builds on existing research by providing empirical data from an actual CubeSat mission MicroOrbiter-1 (MO-1) satellite, which offers valuable insight into the real-world performance of LoRa in space.[12)] By analyzing the effects of the Doppler shift on different Spreading Factors (SF) and examining the relationship between satellite pass elevation and signal degradation, this study aims to contribute to the optimization of LoRa parameters for future LEO satellite missions.

The research compares the performance of the SF7 and SF10 configurations under different Doppler conditions from two ground sensor terminals (GSTs) located in Japan and the United States, providing insight into optimal settings for LEO CubeSat communications. This research contributes empirical data on LoRa performance in LEO environments, which offers significant implications for future CubeSat mission designs, particularly for LoRa-based IoT communication systems.

This paper is organized as follows. The first section provides background research and introduction. The subsequent section discusses the LEO communication background and is followed by the methodology. The paper then presents the results and analysis, and ends with the conclusion.

2. LEO Communication Background

2.1. Doppler effect in LEO

The Low Earth Orbit (LEO) environment presents unique challenges for satellite communication, particularly due to the Doppler effect. The Doppler shift created frequency shifts that can significantly impact signal quality. To accurately model the Doppler shift, orbital mechanics principles and satellite tracking data are utilized. The instantaneous velocity vector of the satellite relative to the GST is calculated, considering parameters such as altitude, inclination, and orbital period. This model allows for the prediction of the variation of the Doppler shift throughout the satelite's orbit.

The Doppler effect can impact the signal-to-noise ratio (SNR) in LoRa transmissions by introducing frequency shifts that may degrade signal quality. Due to its lower processing gain, SF7 is more susceptible to frequency offsets caused by the Doppler effect. This can lead to a decrease in SNR as the receiver may struggle to lock onto the shifted signal, potentially increasing the noise floor relative to the signal power. Meanwhile, SF10 offers a higher processing gain, which helps maintain a better SNR under Doppler conditions. The increased robustness allows the receiver to distinguish the signal from noise more effectively, even with frequency shifts.

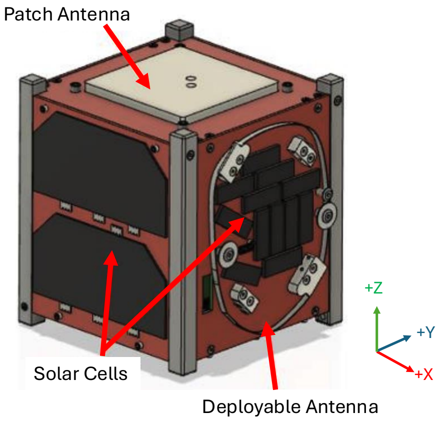

Fig. 1.: MicroOrbiter-1 satellite, with patch antenna for 920MHz LoRa communication, and two deployable dipole antennas for both 400 MHz LoRa mission and UHF non-amateur communications with GS (Uplink at 450 MHz and Downlink at 400.96 MHz).

In LoRa communications, the Doppler effect can lead to frequency offsets that may exceed the receiver's ability to lock onto the signal. It can also affect changes in the chirp rate of LoRa modulation, which can potentially cause demodulation errors. While the time-on-air (ToA) of LoRa packets is a contributing factor to the successful transmission of LoRa communication,[13)] the effect of the Doppler shift would affect this time-critical application.

In general, the Doppler effect can reduce the stability of the signal, potentially lowering the SNR by introducing variability in the received frequency. However, LoRa's Chirp Spread Spectrum (CSS) modulation is designed to be resilient to such effects, especially with higher spreading factors such as SF10.

2.2. MO-1 satellite overview

MO-1 satellite as presented in Fig. 1 is a 1U CubeSat with dimensions of 10 cm x 10 cm x 10 cm with a main mission as Internet of Things (IoT) satellite using LoRa communication to collect sensor data from ground sensor terminals (GSTs) in various places. This form factor imposes strict constraints on the satellite's design, including its power budget, thermal management, and payload capacity. The small surface area of a 1U CubeSat limits the size of the solar panels, resulting in a constrained power budget.

In addition to that, the physical constraints of a 1U CubeSat limit the size of the antennas that can be used for communication. Antennas are selected that provide an optimal balance between size, gain, and radiation pattern. The antenna gain directly affects the link budget, which determines the feasibility of maintaining reliable communication links.

Although MO-1 satellite carried two LoRa communication payloads operating at 400MHz and 920MHz, this paper focuses exclusively on the 920MHz band. The link budget of LoRa transmission of MO-1 satellite that takes into account factors such as free-space loss, antenna gains and system noise temperature is calculated using Eq. (1), with parameters on ground and satellite side elaborated in Table 1 and Table 2 respectively.

Table 1.: Parameters at ground side.

Parameters	Values
Transmission power	250mW (Japan)
	3W (US)
Carrier Frequency	920MHz
Antenna gain	2.15dBi
GST transmission line loss	1dB
Polarization Loss	3dB
Atmospheric + Ionospheric Loss	1.5dB
Orbit	400km

Table 2.: Parameters at satellite side.

Parameters	Values
Antenna pointing loss	3dB
Antenna gain	2.15dBi
Cable loss	1dB
Receiver Sensitivity	-137dB to -140dB[14]

$$P_{rx} = P_{tx} + G_{sys} - L_{sys} - I_{ch} - FSL. \quad (1)$$

3. Methodology

This study uses real LoRa transmission data from the MO-1 satellite, specifically collected from ground sensor terminals (GSTs) in Japan and the United States. These locations were selected due to their similar latitudinal profiles as listed in Table 3, ensuring that the satellite passes exhibit comparable geometric characteristics, particularly in terms of elevation and Doppler shift behavior.

The analysis begins by identifying successful transmission instances from the received datasets. Using the known orbital elements of the MO-1 satellite, the Doppler shift and Doppler rate profiles were computed through MATLAB simulations. The relative radial velocity between the satellite and the GST was projected along the line-of-sight to calculate the Doppler shift at each time step,

$$f_s(t) = \frac{V_{rel}(t)}{c} f_c, \quad (2)$$

where the projection is computed by

$$V_{rel}(t) = \frac{\vec{v}_{rel}(t) \cdot \vec{r}_{rel}(t)}{\|\vec{r}_{rel}(t)\|}, \quad (3)$$

with

$$\vec{v}_{rel}(t) = \vec{v}_{sat}(t) - \vec{v}_{gst}(t), \quad (4)$$

and

$$\vec{r}_{rel}(t) = \vec{r}_{sat}(t) - \vec{r}_{gst}(t). \quad (5)$$

Table 3.: Location of the ground sensor terminals.

	Japan	United States
Latitude [°]	33.8924	38.2138
Longitude [°]	130.84	-77.6579
Terrain Altitude [m]	0.0578	0.0441

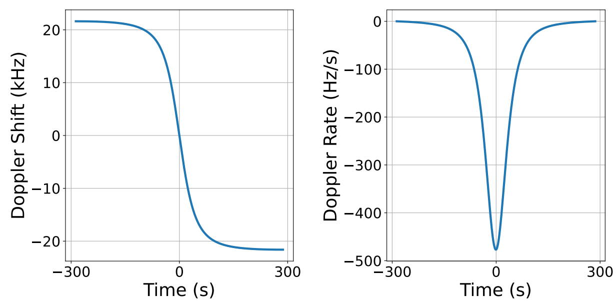

Fig. 2.: Simulation Model of Doppler-shift (left), and Doppler-rate (right) for the satellite pass with maximum elevation of 86.8°.

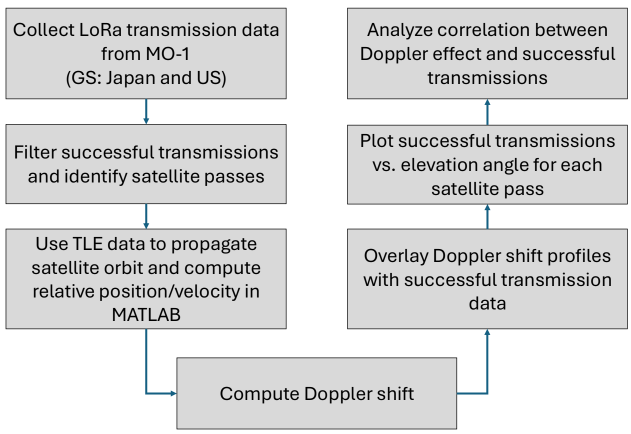

Fig. 3.: Methodology flowchart.

To illustrate this calculation, a simulation of the longest successful transmission pass with a maximum elevation of 86.8° is presented in Fig. 2, representing a 574-second visibility window. For a 920 MHz carrier frequency, the maximum Doppler shift observed in LoRa communication is approximately ±22 kHz, with a corresponding maximum frequency rate of change around ±477 Hz/s.

Subsequently, the number of successful transmissions was plotted against the satellite elevation angles for each pass. This elevation-based mapping enabled visualization of transmission performance across different segments of the pass. By overlaying this information with the simulated Doppler profiles, the study identifies elevation intervals where Doppler effects appear to impact transmission success, revealing the relationship between Doppler dynamics and link reliability in LoRa-based satellite communication. A conceptual overview of this methodology is illustrated in Fig. 3, showing the step-by-step process from data acquisition to Doppler-based transmission analysis.

4. Results and Analysis

The LoRa transmission parameters associated with successful communication with the MO-1 satellite varied by the ground sensor terminal (GST), as summarized in Table 4. This table lists the Spreading Factor (SF), Coding Rate (CR), and Bandwidth (BW) configurations that led to successful receptions from the GST.

Figure 4 presents a plot of the successful LoRa transmission

Table 4.: Successful transmission parameters.

GST Location	SF	CR	BW
Japan	10	4/8	31.25kHz
US	7	4/5	125kHz

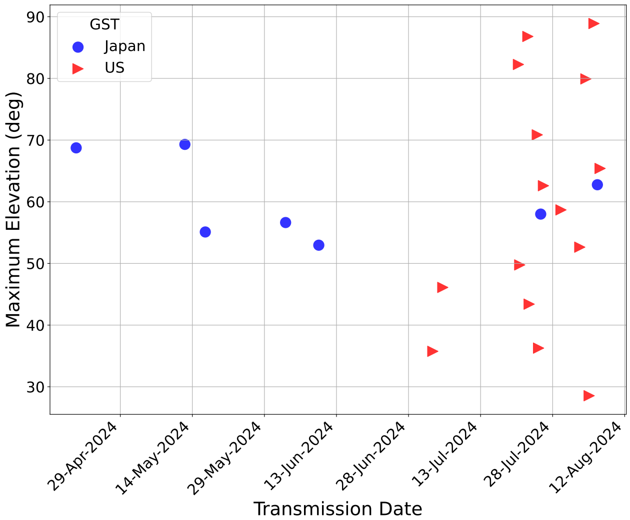

Fig. 4.: Successful LoRa transmission passes observed from Japan and US GSTs, plotted with respect to the maximum elevation of each pass.

passes against the maximum elevation angle observed during each pass. In particular, LoRa communication was successfully achieved at elevation angles as low as 28.5° from the US-based GST. This highlights the LoRa modulation scheme that remains viable at moderate elevation angles despite the increased path loss and Doppler dynamics encountered at lower passes.

As evident in Fig. 4, the Japan GST recorded fewer successful LoRa transmissions, limiting the availability of data for representative analysis in this study. However, we were able to identify four passes with comparable altitude profiles that will be used as the basis for analysis.

In comparison, the US GST recorded a wider range of successful transmissions, allowing greater flexibility in selecting passes with similar altitude characteristics. This selection considers the gradual orbital decay of the satellite over time, which introduces variations in altitude between different passes.

The selected passes to be analyzed with similar altitude profiles for each GST, along with their corresponding maximum elevation angles, and the number of successfully received packets are presented in Table 5. The Doppler shift profiles for each pass from the Japan GST are illustrated in Fig. 5, where the blue lines depict the Doppler shift of each pass and the red lines mark the successful transmissions. Although the small number of successful packets prevents meaningful statistical distribution analysis, the data indicates that LoRa transmissions using SF10 and a 31.25kHz bandwidth remained operational under Doppler shifts reaching up to 19.56kHz. This observation reinforces LoRa's known robustness at higher spreading factors in the presence of significant frequency offsets.[15)]

Further information on the performance at lower elevations is provided in Fig. 6, which maps successful reception times to the elevation angle of the MO-1 satellite over Japan. The detailed

Table 5.: GST-based selected passes.

GST	Pass	Date (2024)	Max. El	Received Packets
Japan	1	12 May	69.3°	6
	2	16 May	55.1°	6
	3	2 Jun	56.63°	2
	4	9 Jun	52.96°	2
US	1	20 Jul	82.26°	27
	2	21 Jul	49.76°	11
	3	22 Jul	86.8°	17
	4	23 Jul	43.4°	9
	5	24 Jul	70.85°	18
	6	26 Jul	62.6°	23

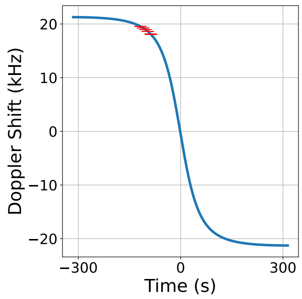

(a) Pass 1

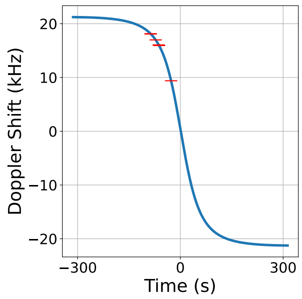

(b) Pass 2

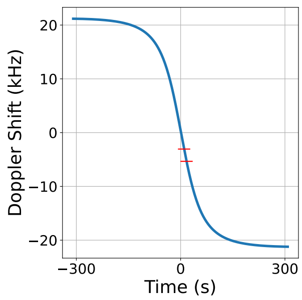

(c) Pass 3

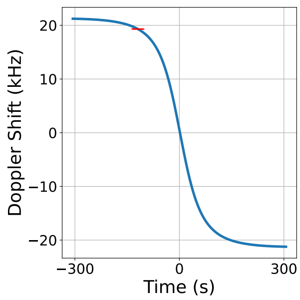

(d) Pass 4

Fig. 5.: Doppler shift plots for selected passes from the Japan GST with successful LoRa transmissions.

results in Table 6 show successful LoRa transmission primarily within the elevation ranges of 20°-30° and 30°-40°. These findings suggest that SF10 with Coding Rate 4/8 and a 31.25kHz bandwidth is particularly suitable for maintaining link reliability during lower-elevation passes, where Doppler shifts are typically more severe.

Table 6.: GST Japan successful LoRa transmission.

Elevation	Successful Transmission			
Range	Pass 1	Pass 2	Pass 3	Pass 4
0-10	0	0	0	0
10-20	0	0	0	2
20-30	6	2	0	0
30-40	0	3	0	0
40-50	0	0	0	0
50-60	0	1	2	-
60-70	0	-	-	-

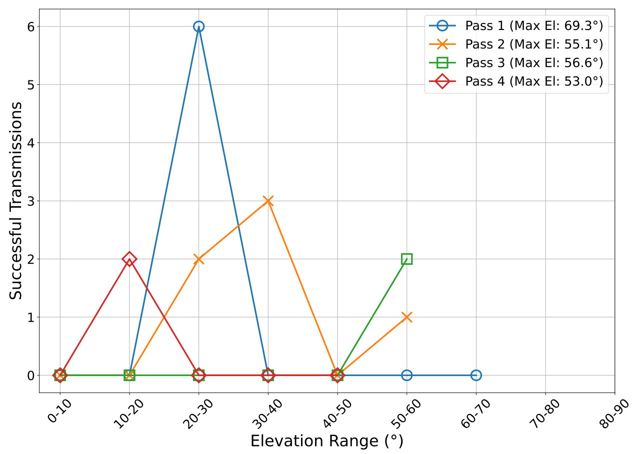

Fig. 6.: LoRa successful transmission vs elevation range of the satellite from GST in Japan.

For US GST transmissions, Fig. 7 depicts Doppler shift profiles overlaid with successful LoRa receptions, where the blue lines illustrate the Doppler shift and the red lines marked the successful transmissions in each pass. The greater volume of successful transmissions from this location enables a clearer pattern identification. Transmission using SF7, with Coding Rate 4/5, and 125kHz bandwidth exhibit strong performance, which aligns with previous research on cross-correlation of the Doppler effect under various LoRa SFs in Ref 16).

The Doppler shift density distribution in Fig. 8 reveals that approximately 58.1% of the successful receptions occurred within a Doppler shift range of ±10.63kHz. In contrast, Doppler shifts that exceeded ±18.83kHz were rarely associated with successful transmission, which only have an occurrence of 2.85%, as detailed in Table 7. The results indicate a threshold beyond which demodulation becomes unreliable, particularly at lower spreading factors.

Figure 9 further characterizes the performance by plotting successful transmissions against the elevation angle of the satellite over the US GST. The majority of successful receptions were observed in the 40°-50° and 50°-60° elevation ranges. These results suggest that satellite passes with peak elevations in the 40° to 60° are optimal for LoRa communication using SF7 and CR 4/5 at 125kHz bandwidth. This is especially relevant for LEO CubeSats in orbits similar to MO-1 (inclination of 51.6°),[17] where these pass geometries frequently occur especially for mid-latitude ground stations.

The analysis presented in this study highlights that LoRa communication performance in LEO satellite scenarios is sig-

Table 7.: Transmission percentage of the Doppler shift range from the US GST.

Doppler Range (kHz)	Occurrence (%)
<-22.25	0
-22.25 to -18.83	1.90
-18.83 to -10.63	14.29
-10.63 to 10.63	58.10
10.63 to 18.83	24.76
18.83 to 22.25	0.95
>22.25	0

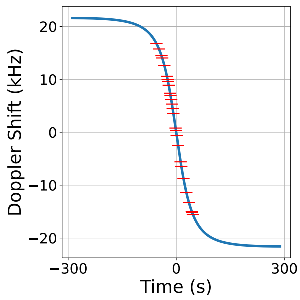

(a) Pass 1

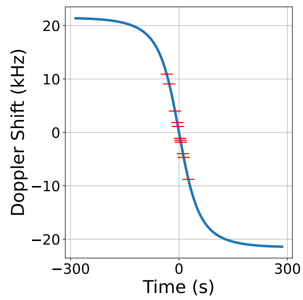

(b) Pass 2

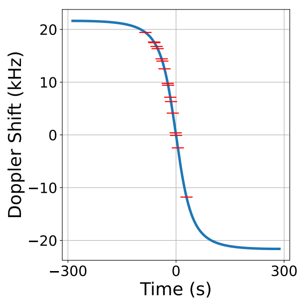

(c) Pass 3

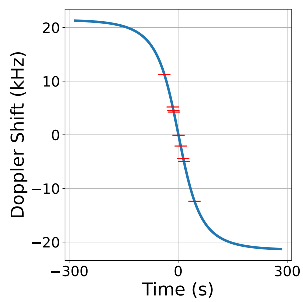

(d) Pass 4

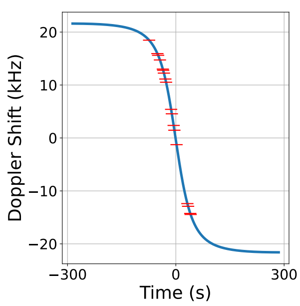

(e) Pass 5

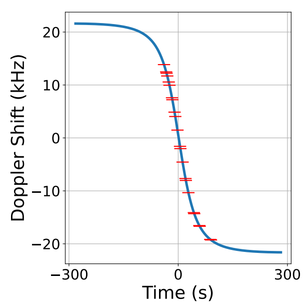

(f) Pass 6

Fig. 7.: Doppler shift plots for selected passes from the US GST with successful LoRa transmissions.

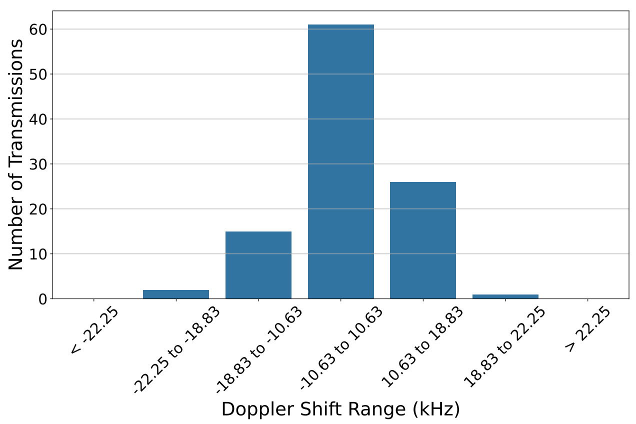

Fig. 8.: Doppler shift density of LoRa transmission from the US GST.

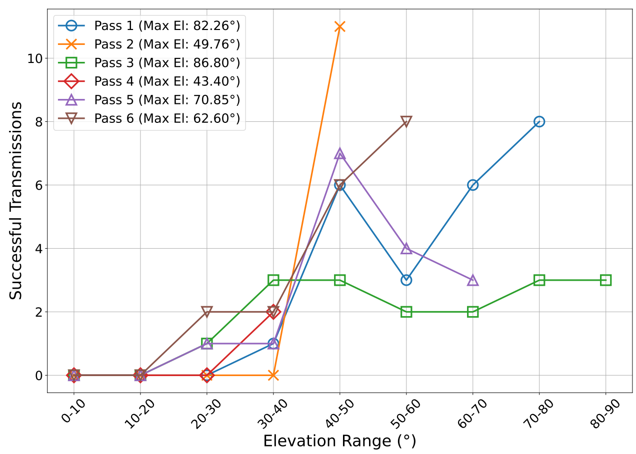

Fig. 9.: LoRa successful transmissions vs elevation range of the satellite from GST in the United States.

nificantly influenced by the Doppler shift and the elevation angle of the satellite pass. The differing success rates between configurations, particularly the superior Doppler resilience of SF10 with narrower bandwidth in low-elevation passes, and the effectiveness of SF7 at moderate elevations with wider bandwidth, suggests that a static parameter configuration may not be optimal throughout all phases of a pass. Instead, adopting an adaptive LoRa parameter strategy, where transmission settings such as Spreading Factor (SF), Coding Rate (CR), and bandwidth (BW) are dynamically adjusted in response to real-time Doppler conditions and link quality, could substantially enhance link reliability and throughput.

Implementing such adaptability would require either preprogrammed switching based on satellite ephemeris predictions or real-time estimation mechanisms based on Doppler shift feedback or received signal power such as RSSI (Received Signal Strength Indicator). The findings of this study provide empirical evidence supporting this strategy, especially for LEO satellites with moderate inclination (51.6°), where pass geometries and Doppler profiles vary widely.

5. Conclusion

This study evaluated the impact of the Doppler shift on LoRa communication in a 1U CubeSat environment, using real transmission data from the MicroOrbiter-1 (MO-1) satellite. The analysis focused on LoRa transmissions from ground sensor terminals (GSTs) in Japan and the United States, utilizing two primary configurations: SF10 with a narrow bandwidth of 31.25kHz and SF7 with a wider bandwidth of 125kHz.

The results confirm that LoRa modulation can maintain reliable communication in space-based applications despite the challenges posed by the Doppler effect, especially when appropriate parameter settings are selected. SF10 with CR 4/8 and 31.25kHz bandwidth was observed and is more robust under higher Doppler shift conditions, typically encountered at lower elevation angles. In contrast, SF7 with CR 4/5 and 125kHz bandwidth exhibited successful performance predominantly at moderate elevation angles (40°-60°), where Doppler conditions are more favorable.

A clear correlation was identified between elevation angle and signal degradation due to the Doppler shift. Passes with maximum elevation angles between 40° and 50° showed the highest success rates, particularly from the US GST. These findings emphasize that the geometry of the satellite pass significantly affects link performance and that moderate elevation passes are optimal to balance coverage duration and Doppler resilience.

Overall, the results demonstrate empirical validation of the viability of LoRa technology for small satellite communications and provide a basis for optimizing LoRa parameters in future LEO satellite missions. The results also underscore that a static parameter configuration is insufficient to ensure optimal performance throughout all orbital phases. Instead, the results advocate for an adaptive communication strategy, such as dynamically adjusting LoRa parameters SF, CR, and BW in real time or based on predicted Doppler and pass geometry.

Future work may explore algorithmic implementations on such adaptive schemes and validate them through on-orbit experiments or hardware-in-the-loop simulations.

Acknowledgments

The author would like to express sincere gratitude to all OB-OG from other projects such as KITSUNE, BIRDS-5, and CURTIS members whose contributions were instrumental to the success of the project: Pooja Lepcha, Fatima Gabriela Duran Dominguez, Tharindu Lakmal Dayarathna Malmadayalage, John Paul Almonte Breta, Pema Zangmo, Giulio Mattei, Mark Angelo Cabrera Purio, Hari Ram Shrestha, Maximilien Berthet, Yudai Etsunaga, Inojosa Andal Raynell, Eliza Sapkota, Kounosuke Nishinaga, and Chinatsu Eto.

Special thanks to the operations team—Linh Ta, Javier Eladio Ferrer Torres, and Ndukayo Zamba Leonel Bakeapai—for their dedicated efforts to ensure the success of satellite transmissions. Also, a heartfelt appreciation goes to our advisors, Hirokazu Masui and Daisuke Nakayama, for their continuous guidance and mentorship throughout the project.

The author is also grateful to our international collaborators: Maulana Ali Arifin, Scott Chapman, Luis Miranda Kunert, Sathit Piluntasopon, Fatimah Zaharah Ali, Mohamad Huzaimy Jusoh, Mohammad Tariqul Islam, Ramson Nyamukondiwa Munyaradzi, and Victor Mukungunugwa, for their valuable support.

Last but not least, we would like to thank JAXA for the launch opportunity.

References

1) Bomani, B. M. M.: CubeSat Technology Past and Present: Current State-of-the-Art Survey, NASA TP-20210000201, 2021.
2) Lepcha P, Malmadayalage TD, Örger NC, Purio MA, Duran F, Kishimoto M, El-Megharbel HA, and Cho M.: Assessing the Capacity and Coverage of Satellite IoT for Developing Countries Using a CubeSat, *Applied Sciences*, **12** (2022).
3) Centenaro, M., Vangelista, L., Zanella, A., and Zorzi, M.: Long-range communications in unlicensed bands: the rising stars in the IoT and smart city scenarios, *IEEE Wireless Communications*, **23** (2016), pp. 60–67.
4) Qu, Z., Zhang, G., Cao, H., and Xie, J.: LEO Satellite Constellation for Internet of Things, *IEEE Access*, **5** (2017), pp. 18391–18401.
5) Haxhibeqiri, J., De Poorter, E., Moerman, I., and Hoebeke, J.: *A Sur-*

vey of LoRaWAN for IoT: From Technology to Application, Sensors, **11** (2018), pp. 1–38.

6) Zadorozhny, A. M., Doroshkin, A. A., Gorev, V. N., Melkov, A. V., Mitrokhin, A. A., Prokopyev, V. Y., and Prokopyev, Y. M.: First Flight-Testing of LoRa Modulation in Satellite Radio Communications in Low-Earth Orbit, *IEEE Access*, **10** (2022), pp. 100006–100023.
7) Colombo, R. M., Mahmood, A., Sisinni, E., Ferrari, P., and Gidlund, M.: Low-cost SDR-based Tool for Evaluating LoRa Satellite Communications, 2022 IEEE International Symposium on Measurements & Networking, Padua, Italy, M&N, 2022, pp. 1–6.
8) Augustin, A., Yi, J., Clausen, T., and Townsley, W. M.: A Study of LoRa: Long Range & Low Power Networks for the Internet of Things, *Sensors*, **9** (2016).
9) Chakravarti, S., Kumar, A. and Tanveer, M.H.: Analysis of the Doppler Effect in Satellite LoRa, Natl. Acad. Sci. Lett., 2024.
10) Ullah, M. A., Pasolini, G., Mikhaylov, K., and Alves, H.: Understanding the Limits of LoRa Direct-to-Satellite: The Doppler Perspectives, *IEEE Open Journal of the Communications Society*, **5** (2024), pp. 51–63.
11) Doroshkin, A. A., Zadorozhny, A. M., Kus, O. N., Prokopyev, V. Y., and Prokopyev, Y. M.: Experimental Study of LoRa Modulation Immunity to Doppler Effect in CubeSat Radio Communications, *IEEE Access*, **7** (2019), pp. 75721–75731.
12) Team, MO-1.: Microorbiter-1 satellite bus system overview, 2022, https://birds-project.com/open-source/pdf/20221207_Microorbiter-1_OpenSourceWebinar.pdf (Accessed May 2025).
13) Khamsah, N. M. N., Moumni, F., Nobayashi, D., Ikenaga, T., and Cho, M.: In-Orbit Performance of LoRa for Internet of Things Communication on MicroOrbiter-1 Satellite, 2024 IEEE International Conference on Communication, Networks and Satellite, Mataram, Indonesia, COMNETSAT, 2024, pp. 48–54.
14) Semtech.: LoRA SX1276/77/78/79 Datasheet, Semtech Corporation, 2015.
15) Semtech.: LoRa Modulation Basics, Application Note AN1200.22, 2015.
16) Deng, J., Benkhelifa, F., and Alouini, M. S.: Orthoganlity analysis in lora uplink satellite communication affected by doppler effect, 2025, https://arxiv.org/abs/2502.16179 (Accessed May 2025).
17) Mission - Customized CubeSat, https://microorbiter.com/ (Accessed May 2025).